Materials Science Advanced Composite Materials
2023 Volume 1, Issue 2
ISSN: 2529-7783

Ultrasonic Vibration Velocity Imaging for Solid Defect Samples Using Laser Probe Method

Yoji Imano, Kazuhiko Imano*

Graduate School of Engineering and Science, Akita University, Akita 010-8502, Japan

***Corresponding author:** Kazuhiko Imano, imano@gipc.akita-u.ac.jp

Abstract

Laser probe method with a constant voltage drive for a piezoelectric transducer is applied to the non-contact ultrasonic imaging method for evaluating defects in a solid sample. The constant voltage driving method for a piezoelectric transducer by the rectangular pulse voltage is the same as our previous papers and can suppress the mechanical ringing of the piezoelectric transducer. The sample to be measured is attached to the vibrating surface of the piezoelectric transducer and is driven by a cycle sinusoidal wave. Ultrasonic wave signal is observed by the laser probe method. Inverse Radon transform is used to obtain the three-dimensional (3D) image after horizontal (2D) projection data acquisitions. As an experimental result, the shape edge of the side wall of the hole in the acrylic disk sample is imaged, and thus the feature and possibilities of detection method for defect are suggested.

Keywords

Ultrasonic imaging
Constant voltage drive
Laser light prob method
Ultrasonic wave
Piezoelectric transducer

1. Introduction

Ultrasonic imaging using the water immersion method often involves immersing the target object in water and receiving reflected waves or transmitted waves from the target object [1]. While this method allows for high-resolution inspections using high-frequency ultrasonic, it poses the risk of degradation deterioration and short-circuiting when electronic devices are placed in water for non-destructive testing. Therefore, it is desirable from the perspective of product reliability to be able to conduct inspections in the air. One method for airborne inspection is to use airborne ultrasonic, but in the air, ultrasound attenuation increases proportionally with frequency, resulting in shorter propagation distances, making high-resolution inspections using high-frequency ultrasound, such as in the MHz range, challenging [2-5].

Our team has previously developed a method for imaging in the air using ultrasound, which utilizes vibration velocity information of ultrasound generated within the target object [6-8]. In this method, a sinusoidal wave vibration, either half or full wave, is generated on a sample placed on a piezoelectric transducer using a constant voltage driving method [6,7]. The vertical vibration velocity of the vibration plane is then used for imaging within the sample, utilizing a laser probe with a narrow beam diameter [9]. However, this method could not achieve significant differences in vibration velocity characteristics between defective and healthy parts within the sample, leading to issues in imaging accuracy.

In contrast, this paper proposes an imaging measurement method that combines the laser probe method and the constant voltage driving method with a CT algorithm [9-13]. In previous methods, laser light was vertically irradiated onto the vibrating sample surface, and imaging images were obtained using the acquired vibration velocity characteristics. In this method, laser light is inject vertically to the direction of ultrasound propagation, and imaging is performed based on the optical information after passing through the sample, using CT algorithm processing. While laser CT have been performed extensively, there are no previous examples of combining the laser probe method and the constant voltage driving method on a piezoelectric transducer, and it is expected to achieve more accurate imaging than conventional measurements using the laser probe method [14].

The measurement procedure involves first contacting a piezoelectric transducer with the transparent solid sample surface to generate planar wave ultrasound inside the sample using constant voltage drive. Subsequently, laser light is directed orthogonally to the ultrasound propagation within the sample, and its transmitted light is received. Since the transmitted light carries both information on deflection due to sound waves and refraction due to the sample shape, it is not possible to correctly image the inside of the sample by scanning it once parallel to the sample surface. Therefore, by using complexified transmitted light information (amplitude values and their phase orthogonally demodulated by a Vector Signal Analyzer, hereafter VSA), a CT algorithm is used to obtain projection images of the sample cross-section. By inverse Radon transforming this image [15,16], imaging images of the target's cross-section are obtained.

In this paper, we first briefly describe the method of generating ultrasound with arbitrary vibration velocity using the constant voltage driving method on the piezoelectric transducer surface. Then, we describe the measurement method of observing the target using this driving method and the CT scan technique, followed by imaging the interior of a transparent sample using the reconstruction method.

2. Piezoelectric transducer driving method

When driving a piezoelectric transducer using a voltage source, the driving voltage waveform and the vibration velocity waveform on the transducer's surface generally do not match. This is because the transducer is an elastic body, and even after the application of voltage to the transducer has ceased, it continues to vibrate as an elastic body. Therefore, in measurement using pulses, ultrasound pulses become longer due to mechanical residual vibrations known as "ringing," which contributes to a decrease in time resolution. To improve this, it is common to use a backing behind the transducer to reduce mechanical Q. In contrast, previous reports have proposed a method that achieves any vibration velocity characteristics by selecting the input voltage waveform to the transducer instead of using a backing to lower the Q value of the transducer [6,8]. This approach allows the generation of ultrasound vibrations without ringing, and is adopted in this paper.

Specifically, the constant voltage driving is achieved by ensuring that the internal impedance of the driving power source is significantly smaller than the impedance of the transducer. Furthermore, the voltage waveform applied to the transducer is set to a rectangular pulse with a time width equal to the transducer's resonance period, $2T$ (T: the time for the wave to propagate in the thickness direction). As a result. the vibration of the frequency component corresponding to $1/2T$ of the driving voltage waveform is reduced, leading to a vibration velocity waveform without ringing [6,8].

Figure 1 represents a system for non-contact measurement of surface vibration velocity of the transducer driven by the aforementioned method using a laser Doppler vibrometer. An oscillator generates rectangular pulse voltage with a pulse width of $2T$ and a repetition period of 100 Hz, which is then amplified up to 100 Vpp using a bipolar amplifier with an output impedance of 0.5 Ω. It is worth noting that the output impedance at the resonance of the piezoelectric transducer is 10 Ω, indicating that constant voltage driving of the transducer is achieved. The transducer used in the experiment was a lead titanate piezoelectric ceramic transducer (Fuji Ceramics, M-6) with a diameter of 40 mm and a thickness of 2.19 mm, and a resonant frequency of 1 MHz (resonant period $2T = 1$ μs).

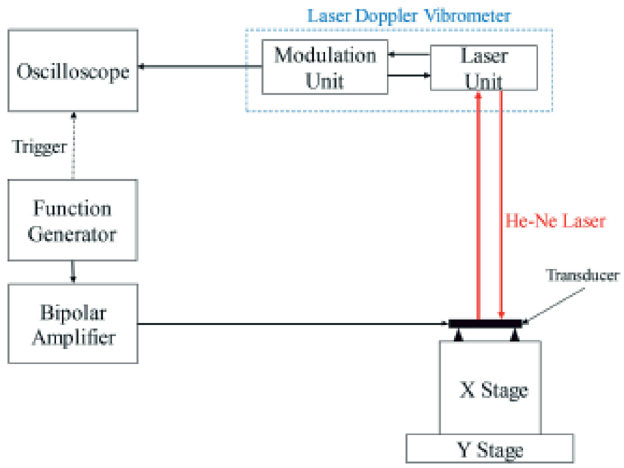

Figure 1. Measurement system for evaluating surface vibration velocity using laser Doppler vibrometer

Figure 2(a) shows the pulse voltage waveform applied to the transducer, with a pulse width of $2T$. **Figure 2(b)** represents the vibration velocity waveform on the transducer's surface. The difference in the rise time of the waveform in **Figure 2(a)** and **Figure 2(b)** (indicated as Td in the figure) is due to a signal delay of about 0.7 μs in the demodulator of the laser Doppler vibrometer. From this figure, it can be seen that an almost one-cycle sinusoidal vibration waveform without ringing is obtained. Additionally, the entire surface of the transducer has an almost flat vibration velocity distribution, and **Figure 2(b)** shows the results at the center of the transducer. This allows for the introduction of a one-cycle planar wave ultrasound, as shown in **Figure 2(b)**, into the sample during imaging, which can suppress multiple scattering within the sample and achieve imaging different from conventional pulse echo methods [8].

3. Imaging

3.1. Imaging methods and samples

Figure 3 illustrates the imaging system proposed in this paper. Additionally, **Figure 4** provides an overview of the sample used in the imaging experiments. The sample is an acrylic plate (30 mm in diameter and 5 mm thick) with a 7 mm diameter hole (simulated defect) as shown in the figure.

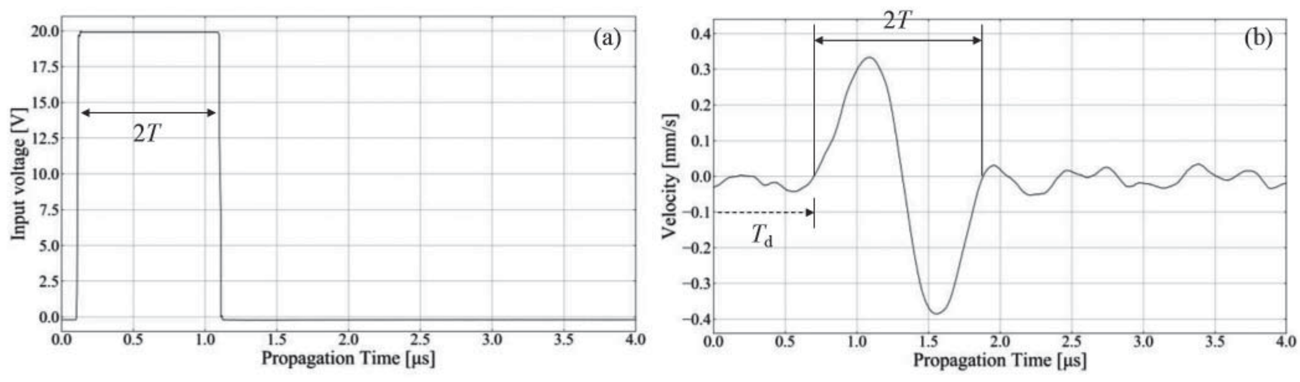

Figure 2. Input rectangular pulse voltage waveform **(a)** and vibration velocity waveform **(b)** measured laser Doppler vibrometer shown in **Figure 1**. This waveform like a one-cycle sinusoidal without ringing can be obtained. (T: Time for wave to propagate in thickness direction).

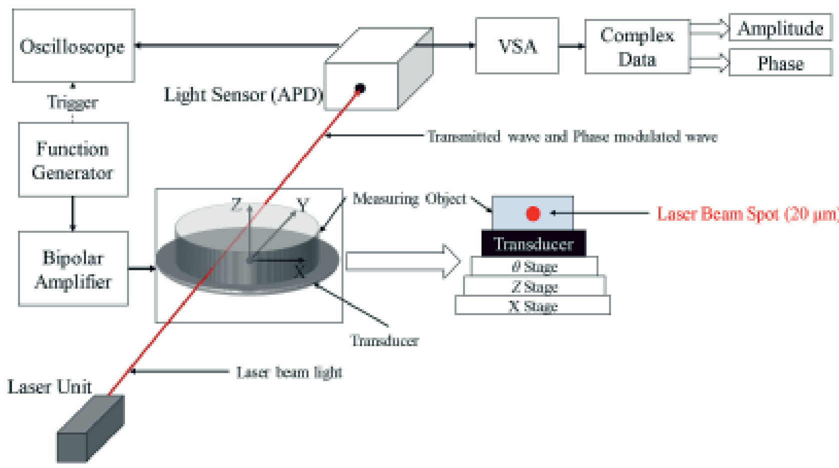

Figure 3. Imaging measurement system using laser probing method

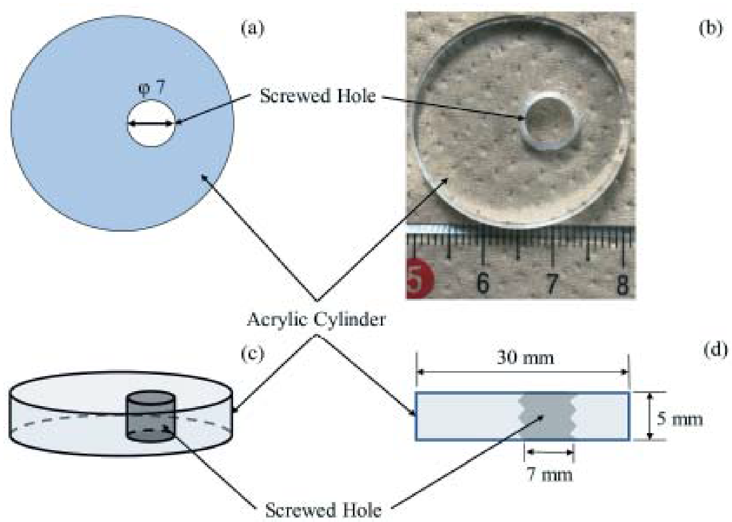

Figure 4. Top view of the imaging sample **(a)**, photo **(b)**, model figure **(c)**, and its side view **(d)**,respectively

To image the target sample, it is securely attached to the surface of the piezoelectric transducer using double-sided tape (water, oil, or grease can also be used), as shown in **Figure 3**. It should be noted that in this measurement method, the thickness of the sample can be chosen arbitrarily. The same ultrasonic transducer as previously described is used. To suppress the ringing of the vibration velocity on the transducer's surface, the applied signal to the transducer is a rectangular pulse voltage with a frequency of 100 Hz, as shown in **Figure 2(a)** (the time width is the reciprocal of the resonance period, $2T$, which is 1 μs).

Firstly, the ultrasonic waves generated by the piezoelectric transducer are propagated in the Z-direction, as shown in **Figure 3**. Furthermore, laser beam light is directed perpendicular to the propagation direction of the ultrasonic waves in the Y-direction, allowing it to pass through the test object. The focus of the laser beam is adjusted to the central part of the test object (laser spot diameter of 20 μm). At this point, the transmitted light is phase-modulated by the ultrasonic waves and is then received by an avalanche photo diode (APD) [9]. During this time, both the unmodulated transmitted light and the phase-modulated wave are simultaneously received on the same sensor's receiving surface and observed through an oscilloscope and vector signal analyzer (VSA), allowing for the observation of amplitude data and phase data. The amplitude values and phase data from this waveform are transferred to a PC via USB.

In addition, this paper utilizes an imaging reconstruction method, and the mentioned measurements are conducted using a CT scanning technique. CT scanning involves measurements of the object from various directions [15], and in this study, CT scanning is performed using laser beam light. Specifically, the center of the transducer (40 mm in diameter) in **Figure 3** is taken as the origin O. The X-Stage is moved in 0.1 mm intervals from X = -20 mm to X = 20 mm, allowing the laser beam light to pass through, repeating the measurements 401 times.

Figure 5 displays the amplitude of the APD output waveform at 1.1 μs after the start of laser beam light incidence for the range of X = -20 mm to 20 mm. From these results, it is evident that the amplitude values (APD output) are higher for the air regions other than the circular sample. Additionally, these values correspond to the stress values (sound pressure) within the material. Next, the θ-Stage is rotated by 6°, and similar measurements are conducted by moving the X-Stage 401 measurements. This measurement is repeated from θ = 0° to θ = 180° with 6° intervals to obtain projection images on the X-Y plane.

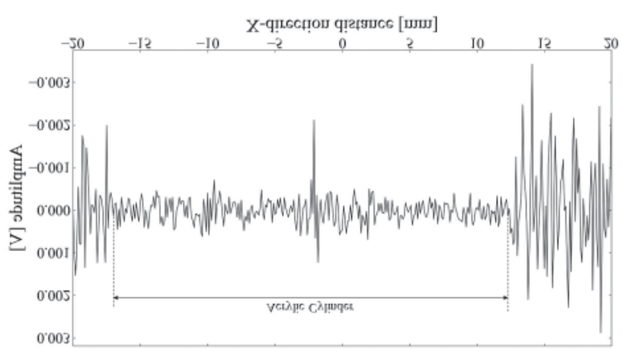

Figure 5. X-direction distance characteristics at propagation time of 1.1 μs

Subsequently, the projection images are processed using the filtered backprojection method (FBP) based on the two-dimensional Fourier transform, which is used for image reconstruction [15,16]. This is a common processing method in current CT scans. The processing flow involves applying a Fourier transform to the projection data and applying a ramp filter. The image can be reconstructed by performing an inverse Fourier transform.

Moreover, for the Z-direction (sample height direction) in **Figure 3**, the Z-Stage is moved in 0.1 mm intervals from Z = 0 mm to Z = 5.5 mm, and similar measurements are repeated. These measurements allow imaging of the ultrasonic propagation characteristics within the sample, enabling the three-dimensional evaluation of defects within the sample.

3.2. Imaging results

Figure 6 displays the projection images of the acrylic sample obtained using the aforementioned method. This image represents a projection image at the center of the thickness of the acrylic sample (Z = 25 mm), with the horizontal axis indicating the number of times the θ-Stage was rotated in steps of 6° (a total of 30 rotations) and the vertical axis indicating the number of times the X-Stage was moved (a total of 401 movements). From this projection image, the position of the hole and the shape of the sample cannot be determined. Therefore, Figure 6's results are subjected to inverse Radon transformation to reconstruct the image and perform imaging.

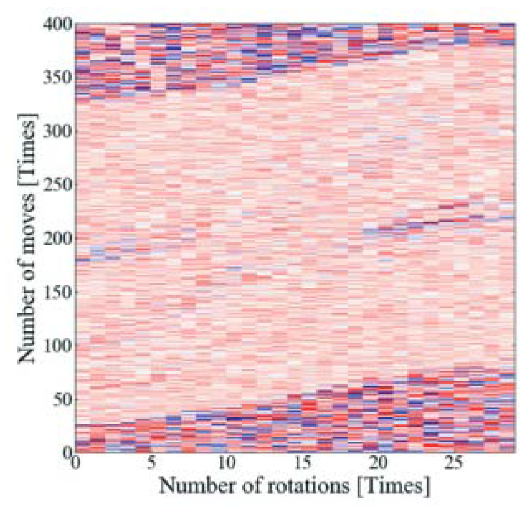

Figure 6. Projected image before imaging

It should be noted that the tilt in the projection image is due to the intentional misalignment of the center (origin) of the transducer and the center of the sample to avoid the influence of soldering on the transducer's part. **Figure 7(a)** is an inverse Radon-transformed image of this projection image, which is the result of imaging in the X-Y plane. Here, the shading in the figure represents the intensity of light received by the APD, and the color is darkest in air. This is because when the laser beam light passes through the sample, some of the light is scattered and the intensity of the light received by the APD is lower than in air. The figure shows that the darker areas correspond to the areas outside the sample (in the air) and the region directly above the piezoelectric transducer. In contrast, the lighter areas correspond to the circular acrylic sample's region. The circular dashed lines in the figure indicate the position of the simulated defect hole. This figure is asymmetrical in the X-direction, as mentioned earlier. This asymmetry is because the center of the transducer and the center of the acrylic circular plate were intentionally offset during installation. Furthermore, variations in the output values in the air and the increased output within the acrylic are due to artifacts resulting from the 6° rotational intervals in the measurements, as evidenced by the regions with straight line (solid circular lines). This artifact can be resolved by reducing the rotational angle during intervals during measurements.

Next, **Figure 7(b)** represents the X-Z plane at Y = 0 mm, which is obtained by stacking the cross-sectional images from Z = 0 mm to Z = 5.5 mm in the Z direction. This image provides an imaging of the sample's cross-section. In the figure, the darker areas represent the cross-section of the acrylic circular plate sample. Additionally, some parts inside the sample show darker areas, indicating the imaging of the simulated defect hole (hollow section). However, the right edge of the hole is not fully imaged, which is attributed to measurement being conducted by varying the θ-Stage from 0° to 180° (half-circle). This can be resolved by extending the measurements to cover a full 360° rotation. Thus, three-dimensional measurements enable the determination of the depth of defects.

Furthermore, **Figure 8** depicts the imaging results in the X-Y plane at Y = 2.5 mm after the propagation of ultrasonic waves (without ultrasound irradiation). As demonstrated, since the imaging in this paper is based on interactions with ultrasound, imaging cannot be performed in areas where there is no interaction.

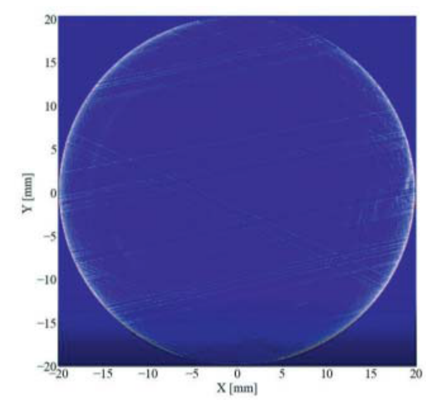

Figure 8. XY plane imaging results after ultrasonic propagation (without ultrasonic irradiation)

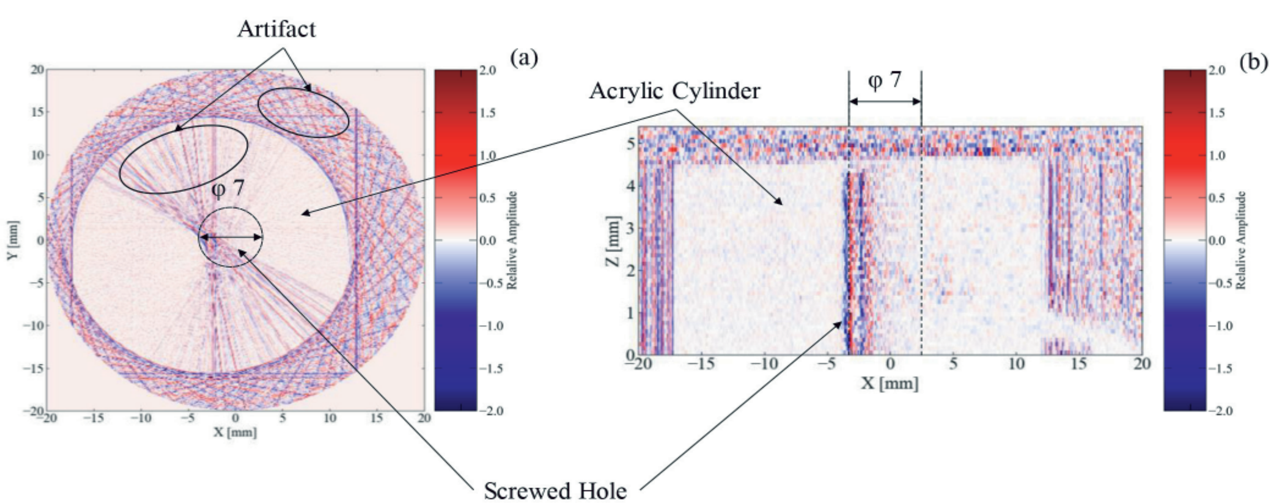

Figure 7. The imaging results in XY plane **(a)** and XZ plane **(b)**

In conclusion, the ultrasonic imaging method proposed in this paper has the potential to serve as a measurement technique for detecting defects inside transparent material samples such as glass and acrylic resin.

4. Conclusion

In this paper, we discussed a method for imaging air-filled defects inside transparent solid samples (acrylic circular plate) by introducing ringing-free planar ultrasonic waves into the sample using an ultrasonic piezoelectric transducer (frequency: 1 MHz) and utilizing information obtained from the deflection of the laser beam light used as a probe by the internal ultrasonic waves. As a result, we demonstrated that the proposed measurement technique can image the internal structure of the sample to some extent in both two-dimensional and three-dimensional forms, thereby revealing the potential for defect detection. Currently, driving the ultrasonic transducer at a constant voltage does not provide ultrasonic waves of sufficient intensity, posing challenges in terms of dynamic range and signal-to-noise (S/N) ratio. In the future, we plan to explore different driving conditions for the ultrasonic transducer (e.g., using multiple sinusoidal wave signals), improve signal processing to obtain amplitude images, phase images, and complex amplitude images, and apply this measurement method to samples with varying shapes and acoustical properties to establish a novel imaging approach.

Disclosure statement

The authors declare no conflict of interest.

References

[1] Ultrasound Compendium Committee. Ultrasound Compendium, 1999, Maruzen Co. Ltd., p. 364.

[2] Imano K, Nishihira M, Sasaki K, 2005, Lateral Resolution Beyond Diffraction Limit Using 40 kHz Air-Coupled Ultrasonic Systems. Electron Lett, 41(10): 620–622.

[3] Sasaki K, Nishihira M, Imano K, 2006, Low-Frequency Air-Coupled Ultrasonic System Beyond Diffraction Limit Using Pinhole. Jpn J Appl Phys, 45(5B): 4560–4564.

[4] Imano K, Kondou M, 2008, Possibilities of Nondestructive Evaluation of a Pipe Using Air-Coupled Ultrasonic Wave in the MHz Range. IEICE Electronics Express, 5(17): 668–671.

[5] Imano K, Kondou M, 2009, Detecting Pipe Wall Reduction Using Air-Coupled MHz Range Ultrasonic Wave. IEICE Electronics Express, 6(10): 613–617.

[6] Imano K, Sato H, 2013, A Method for Ultrasonic Imaging Using Vibration Velocity Information. Journal of the Society of Materials Engineering for Resources of Japan, 25(1/2): 14–19.

[7] Imano K, 2018, Ultrasonic Imaging of Thin Plate Samples Using Vibration Velocity Information Wave Imaging. Journal of the Imaging Society of Japan, 57(4): 422–425.

[8] Imano K, 2014, Barker-Coded Ultrasonic Imaging Using Optical Surface Vibration Measurement. Journal of the Imaging Society of Japan, 53(6): 476–479.

[9] Imano K, 2015, Ultrasonic Sound Field Observation Using Laser Light as a Probe for Field Observation. Japanese Journal of Optics, 44(12): 488–493.

[10] Imano K, 2016, One Method of Second Harmonic Ultrasonic Detection of Internal Cracks in Solid Samples Using Optical Deflection Method. Journal of the Society of Materials Engineering for Resources of Japan, 27(1/2): 6–9.

[11] Akatsuka M, Imano K, 2019, Relationship Between Rayleigh Wave Phase and Residual Stress on Tempered Glass Surface by Laser Probing Method. Journal of the Society of Materials Engineering for Resources of Japan, 30(1/2): 23–26.

[12] Imano K, Akatsuka M, 2019, Relationship Between Residual Stress and Ultrasonic Phase in a Small Region in PMMA. Journal of the Society of Materials Engineering for Resources of Japan, 30(1/2): 18–22.

[13] Imano K, Akatsuka M, 2019, One Evaluation Method of Residual Stress in Solid Samples by Probing Ultrasonic Propagation Using Laser Light. Journal of the Society of Materials Engineering for Resources of Japan, 30(1/2): 6–10.

[14] Enomoto M, Devaraj B, Kobayashi M, et al., 1998, Study on Laser Optical CT Imaging Measurement of Human Teeth by Coherent Detection Imaging Method. Nippon Laser Igakkaishi, 19(1): 1–12.

[15] Takagi M, Shimoda Y. Handbook of Image Analysis, 1991, University of Tokyo Press, p. 356–370.

[16] Hashimoto Y, Shinohara H. Basics of Image Reconstruction in C, 2006, Medical Science, p. 248–253.